Structure determination of the silver carboxylate dimer $[Ag(O_2C_{20}H_{39})]_2$, silver arachidate, using powder X-ray diffraction methods

Peter W. Stephens,[1] James A. Kaduk,[2] Thomas N. Blanton,[3,a)] David R. Whitcomb,[4] Scott T. Misture,[5] and Manju Rajeswaran[3]

[1]*Department of Physics and Astronomy, Stony Brook University, Stony Brook, New York 11794–3800*
[2]*Illinois Institute of Technology, 3101 S. Dearborn, Chicago, Illinois 60616*
[3]*Research Laboratories, Eastman Kodak Company, Rochester, New York 14650–2106*
[4]*Carestream Health, 1 Imation Way, Oakdale, Minnesota 55128*
[5]*New York State College of Ceramics, Alfred University, Alfred, New York 14802*

(Received 13 February 2011; accepted 27 February 2011)

High-resolution powder X-ray diffraction and density functional plane wave pseudo-potential techniques have been used to obtain an optimized structural model of silver arachidate, $[Ag(O_2C(CH_2)_{18}CH_3]_2$. The unit cell is triclinic, space group $P\text{-}1$ with cell dimensions of $a = 4.1519(10)$ Å, $b = 4.7055(10)$ Å, $c = 53.555(4)$ Å, $\alpha = 89.473(15)°$, $\beta = 87.617(5)°$ and $\gamma = 76.329(5)°$. The structure is characterized by an 8-membered ring dimer of Ag atoms and carboxyl groups joined by four-member Ag–O rings with fully extended zigzag side chains, giving rise to one-dimensional chains along the *b*-axis. © *International Centre for Diffraction Data* [doi:10.1017/S0885715612000309]

Key words: silver arachidate, silver carboxylate, structure determination, X-ray diffraction

I. INTRODUCTION

The silver source in thermal and photothermal dry imaging media is reducible silver carboxylates (Morgan, 1991). Although a number of silver carboxylate complexes have been evaluated for dry-silver imaging applications, the simpler fatty acids have been found to be the primary ligands of choice in commercial applications (Cowdery-Corvan and Whitcomb, 2002). These fatty acid silver salts typically comprise 8-membered dimer rings, schematically illustrated in Figure 1 (Wu and Mak, 1995).

A recent crystal structure determination of silver behenate concluded that the 8-membered dimer rings are connected by four-membered Ag–O rings giving rise to a one-dimensional polymeric network (Blanton *et al.*, 2011). This structure-type results in diffraction patterns with a series of uniformly spaced (in $\sin\theta$) low-angle diffraction peaks that can be used to calibrate a diffractometer (Blanton *et al.*, 1995). The X-ray diffraction patterns in Figure 2 for silver arachidate, $[Ag(O_2C_{20}H_{39})]_2$, silver behenate $[Ag(O_2C_{22}H_{43})]_2$ and silver mellisate $[Ag(O_2C_{30}H_{59})]_2$ demonstrate the increase in long-period $d(001)$ spacing with fatty acid chain length.

Single-crystal analysis is the preferred method for structure elucidation when suitable samples are available. However, the inability to grow single crystals with adequate size and quality of silver arachidate (AgAra) has prevented the use of this technique to determine the AgAra structure. Powder XRD patterns of commercially available AgAra show this silver carboxylate to be crystalline; however, the diffraction peaks are too broad for indexing the diffraction pattern. In this study, AgAra has been successfully recrystallized, producing large particles that combined with a high-resolution diffractometer, synchrotron radiation and density functional plane wave pseudo-potential techniques have been used to obtain an optimized structural model of silver arachidate.

II. EXPERIMENTAL

A. Sample preparation

Arachidic acid (Kodak) was dispersed in water at a few percent concentration and then heated to approximately 85 °C. An equivalent amount of sodium hydroxide in water was added to make sodium arachidate. The temperature was dropped to 50–55 °C followed by the addition of an aqueous solution of silver nitrate. A white precipitate of AgAra was stirred for 1 h, then filtered and washed with water twice. The collected solids were air dried until all water evaporated. AgAra prepared in this manner was composed of platelets ~0.1-μm-thick and 0.5–1 μm in the plane of the sample. After drying, the AgAra was recrystallized by slow cooling a hot (~70–75 °C) filtered solution of 1.0 g AgAra in 200 ml ethanol:pyridine (10:1 v/v). The resulting particles were also observed to be platelets (Figure 3) with a thickness of ~1 μm and planar dimension of 20–30 μm.

B. High-resolution synchrotron radiation diffraction

High-resolution powder diffraction data were collected on the SUNY X16C beamline at the National Synchrotron Light Source, Brookhaven National Laboratory. The direct synchrotron beam was monochromated by a double Si(111) crystal tuned to a wavelength of 0.70052(1) Å. The diffracted beam was reflected by a Ge(111) analyzer crystal into a NaI scintillation counter. Diffraction data were collected at room temperature from 0.50° to 29° (*d*-spacing from 80.27 to 1.399 Å) with a count time increasing from 2 to 20 s/point.

a) Electronic mail: thomas.blanton@kodak.com

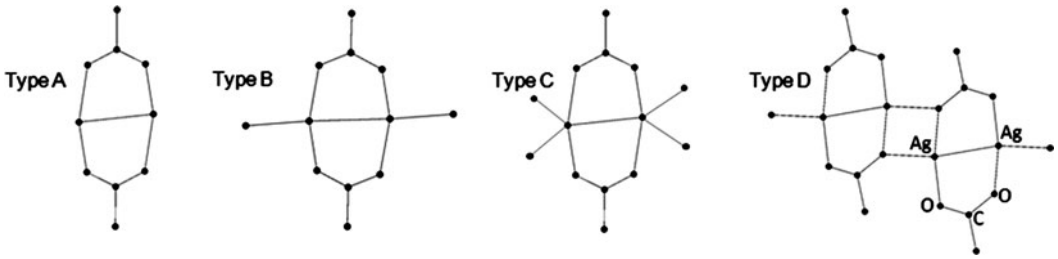

Figure 1. Schematic of Type A–D dimer structures of silver carboxylates.

C. Structure model determination

Elucidation of the crystal structure model from high-resolution powder diffraction data followed a series of steps applied in a systematic approach:

1. Unit-cell indexing using manual zone by zone-axis evaluation with TOPAS and TOPAS-Academic (Bruker AXS, 2005; Coelho, 2007).
2. Peak profile fitting for peak position and intensity using Pawley refinement (Pawley, 1991).
3. Structure solution using PSSP (Pagola and Stephens, 2010).
4. Structure refinement using TOPAS.
5. Density functional geometry optimization using CASTEP (Clark *et al.*, 2005)

III. RESULTS AND DISCUSSION

The high-resolution powder diffraction pattern of AgAra is shown in Figure 4. The first step in structure solution from powder diffraction data is to index the unit cell, *i.e.* to find a lattice that permits the assignment of Miller indices (*hkl*) to each observed peak, within the error of measurement. While, in general, indexing is a routine task using established computer programs if data of the present quality are available, the large disparity between unit-cell parameters renders it difficult in this case. In particular, the (*hk0*) zone, which is required to establish the unit-cell parameters, first appears at the 54th allowed peak, the (110) at $2\theta = 11.63°$. Many iterations of indexing using commercially available programs yielded candidate lattices, but none of them resulted in a profile fit sufficiently better than others to determine the lattice decisively. With such a large number of closely spaced diffraction peaks, the profile fits were highly metastable. Ultimately, we used the following procedure based on the fact that the *c*-axis is much longer than *a* and *b*, so that the reciprocal lattice vectors *a** and *b** are very much longer than *c**, and can be chosen to be nearly perpendicular to *c**. This approach means that in a powder pattern, each peak (*hk*0) will be the source of a series of closely spaced peaks extending to higher angles.

The first 11 diffraction peaks can be indexed as (001) to (0011). The first peak that could not be indexed as (00*l*) at 8.78° provided an estimate for *b**, and the correct assignment of any two peaks in that region sets *b** and reciprocal lattice angle α^*. In the present case, assigning indices (012) to the strong peak at 8.91° allowed indexing of all peaks below 10°. Assignment of *a** and reciprocal lattice angle β^* is less

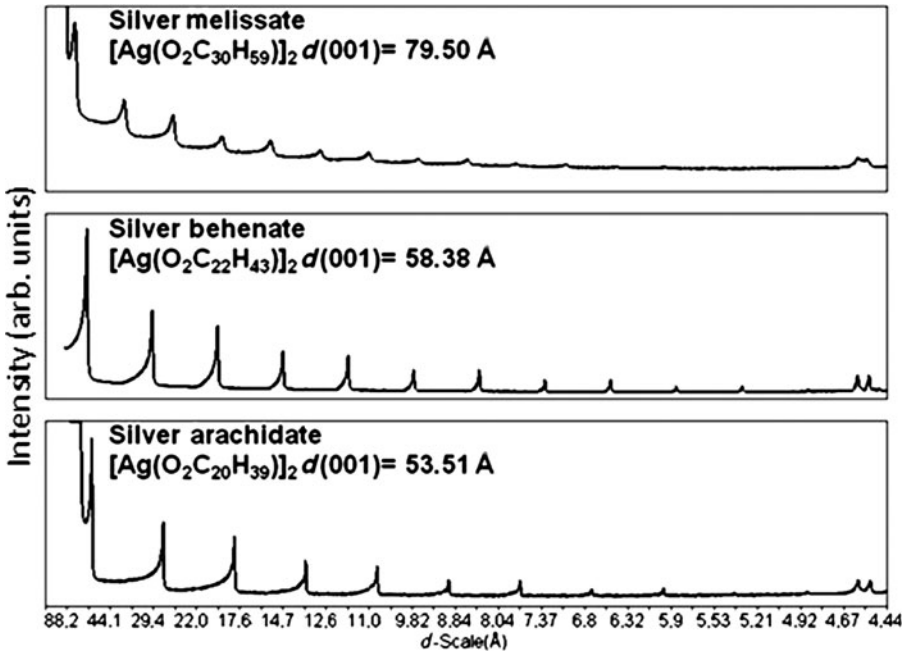

Figure 2. Low-angle powder X-ray diffraction patterns for recrystallized silver arachidate, $Ag(O_2C_{20}H_{39})]_2$, recrystallized silver behenate $Ag(O_2C_{22}H_{43})]_2$ and silver mellisate $Ag(O_2C_{30}H_{59})]_2$ showing (00*l*) diffraction peaks. Collected using synchrotron radiation.

https://doi.org/10.1017/S0885715612000309 Published online by Cambridge University Press

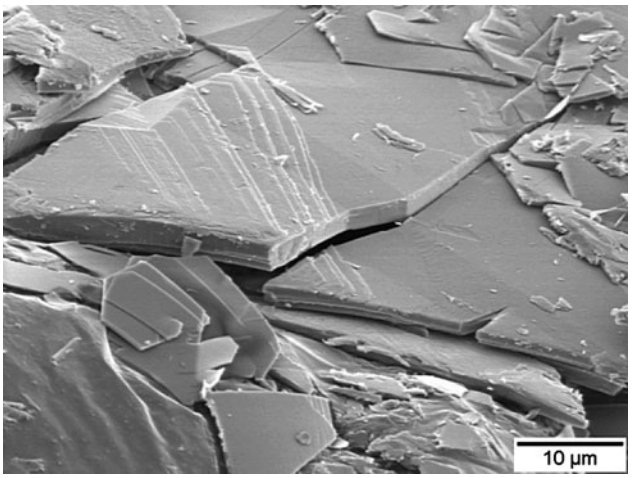

Figure 3. Scanning electron micrograph of AgAra recrystallized in ethanol: pyridine.

immediately obvious because the (101), (100) and (101) peaks are relatively weak, but careful examination of the diffraction pattern in the range of 9–12.5° found the indexing to be correct. To establish reciprocal lattice angle γ^*, one has to correctly assign one peak in the (11l) series. All the (11l) peaks are noticeably broader than the other peaks, suggesting that anisotropic strain is present, which gives rise to some ambiguity in the assignment (this broadening was modeled in the profile fitting and refinement stages by an extra parameter, adding a Lorentzian strain term to peaks with h and k both non-zero). Finally, the most prominent peak not assigned in the first two zones turns out to be the (113) at 11.78°. This assignment was subsequently confirmed by the structure model. At each stage of indexing, TOPAS was used to compute a Pawley fit of the pattern to a lattice containing the established zones, and to fit the positions of the unindexed peaks to predict the reciprocal lattice parameters of the next zone to be included. A final Pawley fit was carried out, establishing a set of intensities and correlation coefficients, used as input to the real-space simulated annealing structure solution program PSSP. Using correlated estimates of intensities is known to be important in handling overlapped peaks in powder diffraction patterns (David *et al.*, 1998).

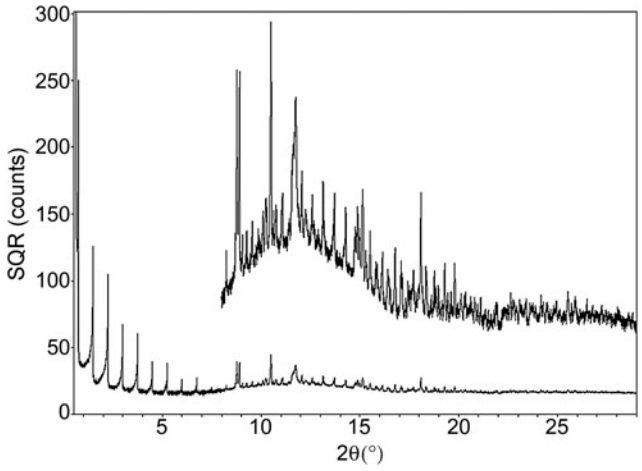

Figure 4. High-resolution powder X-ray diffraction pattern of recrystallized AgAra collected using 0.70052(1) Å synchrotron radiation. Intensity plotted as square root counts for better visualization of low-intensity peaks.

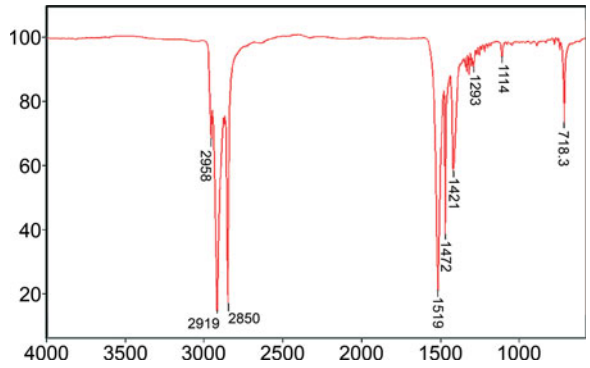

Figure 5. (Color online) IR spectrum of AgAra.

Lee *et al.* (2002) have described the IR spectra for silver stearate. Accordingly, assignments to the major IR bands of AgAra (Figure 5) are made.

The band at 718 cm^{-1} is the CH_2 rocking vibration, the bands at 1421 and 1519 cm^{-1} are assigned to the symmetric and anti-symmetric stretching vibrations of the carboxylate group. Note the lack of a strong band at 1700 cm^{-1}, indicating the absence of C = O that would be due to COOH. The single band at 1472 cm^{-1} suggests that AgArachidate exists in a triclinic cell with a single type of alkyl chain per subcell. The two bands observed at 2850 and 2919 cm^{-1} are assigned to the symmetric ($\nu_s(CH_2)$d+) and asymmetric ($\nu_{as}(CH_2)$d−) stretching vibrations of the methylene groups, respectively. The small bandwidth of 1472 cm^{-1}, and the location of the 2850 and 2919 cm^{-1} bands are indicative of a highly ordered all-trans configuration of the alkyl chains.

Based on XRD and IR data, and Ag carboxylate chemistry, and similarity to the previously solved AgBehenate structure, a preliminary structural model comprising an 8-membered dimer ring with an all-trans aliphatic chain for AgArachidate was proposed. In this model, the 8-membered dimer rings in neighboring molecules are connected in a polymeric-like network by four-member rings of Ag and O, referred to as a "type D" dimer structure for silver (I) carboxylate complexes. However, Rietveld refinements of this model were unstable and resulted in implausible bond distances. This result is likely due to the fact that reflections contributing to the refinement all had $|h|$ and $|k| \leq 1$, so the atoms were poorly triangulated in the a–b-plane.

The next approach was to optimize the preliminary AgArachidate structure model (fixed unit cell) using density functional plane wave pseudo-potential techniques as implemented in CASTEP. The Perdew–Wang 91 functional was used, with a 340-eV plane wave basis set cut-off. The Brillouin zone was sampled using 15 k-points. The density functional theory calculation results indicate that the charge in the Ag ion is +0.80, and the charges on the oxygen atoms are −0.55 and −0.58. The Mulliken overlap populations:

Ag1–O2	2.207 Å	0.21e
Ag1–O1(8-membered ring)	2.348 Å	0.22e
Ag1–O1(4-membered ring)	2.629 Å	0.05e

https://doi.org/10.1017/S0885715612000309 Published online by Cambridge University Press

Table I. Crystal data for AgAra

Empirical formula	$C_{20}H_{39}AgO_2$	
Formula weight	419.4	
Crystal system	Triclinic	
Space group	*P*-1	
Unit cell dimensions	$a = 4.1519(10)$ Å	$\alpha = 89.473(15)°$
	$b = 4.7055(10)$ Å	$\beta = 87.617(5)°$
	$c = 53.555(4)$ Å	$\gamma = 76.329(5)°$
Volume	1015.8(3) Å^3	
Z	2	
Density (calculated)	1.371 kg/m^3	

Table II. Selected bond distances (Å) and bond angles (°) for AgAra

Ag1A–Ag2A	2.746	O1(a)–Ag1A–O2	112.77
Ag1A–O2	2.201	O1(a)–Ag1A–O1(b)	78.65
Ag1A–O1(a)	2.239	Ag1A–O1(a)–C1	127.59
Ag1A–O1(b)	2.393	O1(a)–C1–O2	124.33
O1–C1	1.288		
O2–C1	1.271		

(a) O1 in 8-membered ring.
(b) O1 in 4-membered ring.

indicate that the Ag–O bonds have significant covalent character. The highest energy occupied states (highest occupied molecular orbit (HOMO)) consist of mixtures of Ag d and O p orbitals. The lowest energy unoccupied states (lowest unoccupied molecular orbit (LUMO)) are Ag d orbitals.

The details of the AgAra structure model unit-cell data are summarized in Table I, selected geometric parameters are shown in Table II, and atomic co-ordinates are listed in Tables III and IV.

The overall conformation and its atomic numbering scheme are shown in Figure 6(a). As expected from the proposed structural model, Figure 6(b) illustrates an 8-membered ring dimer of Ag atoms and carboxyl groups joined by four-membered Ag–O rings with fully extended zigzag side chains, giving rise to a one-dimensional polymeric network in the *bc*-plane of the unit cell, viewed along the *x*-axis.

The close interaction (2.809 Å) between two Ag atoms in the 8-membered ring dimers is not unusual for silver carboxylate structures (Chen and Mak, 1991; Jaber *et al.*, 1996; Olson *et al.*, 2006; Whitcomb and Rajeswaran, 2006), and consistent with the EXAFS 2.8 Å Ag–Ag distance observed for AgBehenate (Blanton *et al.* 2007).

IV. SUMMARY

The crystal structure of silver arachidate has been proposed. Unable to use standard single-crystal techniques, a synergistic combination of (1) optimal AgArachidate powder

Table III. Final coordinates and equivalent isotropic displacement parameters of the non-hydrogen atoms for AgAra.

Atom	*x/a*	*y/b*	*z/c*	*U* (Å^2)
Ag1	0.2423	−0.1745	0.0137	0.0475
O1	−0.3505	0.3925	0.0237	0.0475
O2	0.0050	0.0693	0.0471	0.0475
C1	−0.2269	0.2974	0.0447	0.0475
C2	−0.3653	0.4753	0.0677	0.0475
C3	−0.4197	0.2953	0.0907	0.0475
C4	−0.5695	0.4896	0.1129	0.0475
C5	−0.6396	0.3200	0.1361	0.0475
C6	−0.7842	0.5157	0.1583	0.0475
C7	−0.8628	0.3488	0.1814	0.0475
C8	−1.0108	0.5469	0.2035	0.0475
C9	−1.0872	0.3823	0.2268	0.0475
C10	−1.2230	0.5814	0.2490	0.0475
C11	−1.2941	0.4177	0.2725	0.0475
C12	−1.4237	0.6167	0.2949	0.0475
C13	−1.4940	0.4524	0.3183	0.0475
C14	−1.6226	0.6505	0.3408	0.0475
C15	−1.6951	0.4850	0.3641	0.0475
C16	−1.8280	0.6825	0.3864	0.0475
C17	−1.9024	0.5171	0.4097	0.0475
C18	−2.0506	0.7165	0.4316	0.0475
C19	−2.1168	0.5528	0.4552	0.0475
C20	−2.2631	0.7562	0.4769	0.0475

Table IV. Hydrogen atom positions and isotropic displacement parameters for AgAra.

Atom	*x/a*	*y/b*	*z/c*	*U* (Å^2)
H2a	−0.1890	0.6097	0.0717	0.0475
H2b	−0.5969	0.6303	0.0631	0.0475
H3a	−0.5849	0.1537	0.0861	0.0475
H3b	−0.1824	0.1493	0.0956	0.0475
H4a	−0.4027	0.6304	0.1176	0.0475
H4b	−0.8021	0.6402	0.1075	0.0475
H5a	−0.4087	0.1659	0.1414	0.0475
H5b	−0.8110	0.1834	0.1315	0.0475
H6a	−1.0124	0.6722	0.1528	0.0475
H6b	−0.6108	0.6497	0.1631	0.0475
H7a	−0.6346	0.1937	0.1871	0.0475
H7b	−1.0347	0.2135	0.1766	0.0475
H8a	−1.2395	0.7015	0.1978	0.0475
H8b	−0.8388	0.6829	0.2081	0.0475
H9a	−0.8594	0.2238	0.2321	0.0475
H9b	−1.2646	0.2506	0.2224	0.0475
H10a	−1.4520	0.7390	0.2438	0.0475
H10b	−1.0457	0.7141	0.2531	0.0475
H11a	−1.0656	0.2582	0.2776	0.0475
H11b	−1.4739	0.2870	0.2685	0.0475
H12a	−1.6524	0.7763	0.2899	0.0475
H12b	−1.2437	0.7471	0.2989	0.0475
H13a	−1.2655	0.2924	0.3233	0.0475
H13b	−1.6743	0.3223	0.3144	0.0475
H14a	−1.8505	0.8114	0.3358	0.0475
H14b	−1.4417	0.7794	0.3449	0.0475
H15a	−1.4670	0.3252	0.3692	0.0475
H15b	−1.8743	0.3547	0.3599	0.0475
H16a	−2.0559	0.8420	0.3813	0.0475
H16b	−1.6494	0.8131	0.3908	0.0475
H17a	−1.6726	0.3643	0.4154	0.0475
H17b	−2.0731	0.3795	0.4052	0.0475
H18a	−2.2841	0.8654	0.4261	0.0475
H18b	−1.8834	0.8586	0.4358	0.0475
H19a	−1.8835	0.4040	0.4608	0.0475
H19b	−2.2848	0.4114	0.4512	0.0475
H20a	−2.5008	0.9021	0.4722	0.0475
H20b	−2.0965	0.8953	0.4817	0.0475
H20c	−2.3079	0.6347	0.4938	0.0475

https://doi.org/10.1017/S0885715612000309 Published online by Cambridge University Press

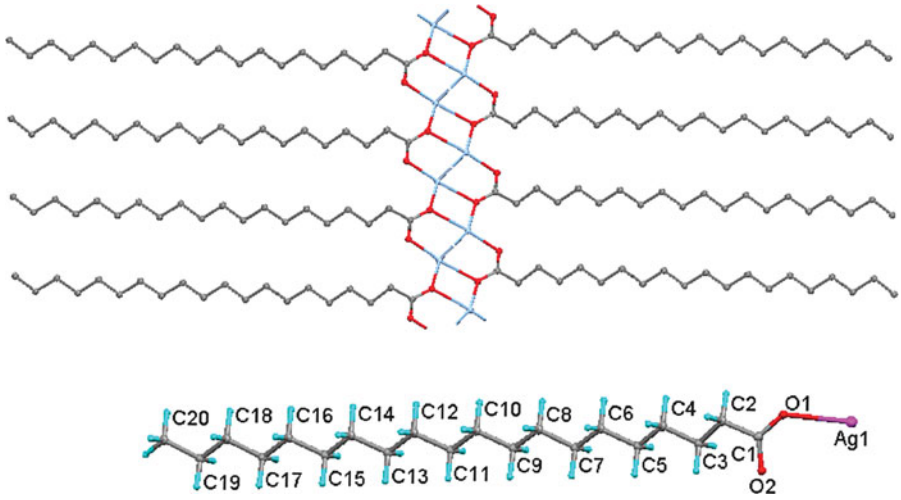

Figure 6. (Color online) (a) Bottom: conformation of AgAra, with the atomic numbering scheme. (b) Top: unit-cell packing in AgAra sheets in the *b*–*c*-plane.

sample, (2) high-resolution synchrotron radiation powder data and (3) density functional structure optimization was necessary to carry out structure determination. Two AgArachidate molecules form an 8-membered ring dimer composed of two Ag atoms and two carboxyl groups with dimers joined by four-member Ag–O rings, creating a one-dimensional polymeric network. The remaining C_{19} alkyl chains were modeled with trans configuration. These results also agree with IR data and known silver carboxylate structures, supporting the structure model.

ACKNOWLEDGMENTS

The authors thank Sharon Markel (Eastman Kodak Company) for collection of IR data. Use of the National Synchrotron Light Source, Brookhaven National Laboratory, was supported by the U.S. Department of Energy, Office of Science, Office of Basic Energy Sciences, under Contract No. DE-AC02-98CH10886.

Blanton, T. N., Huang, T. C., Hubbard, C. R., Robie, S. B., Louer, D., Gobel, H. E., Will, G., Gilles, R., and Raftery, T. (**1995**). "JCPDS-International Centre for diffraction data round robin study of silver behenate: a possible low-angle X-ray diffraction calibration standard," Powder Diff. **10**, 91–95.

Blanton, T. N., Whitcomb, D. R., and Misture, S. T. (**2007**). "An EXAFS study of photographic development in thermographic films," Powder Diff. **22**, 122–125.

Blanton, T. N., Rajeswaran, M., Stephens, P. W., Whitcomb, D. R., Misture, S. T., and Kaduk, J. A. (**2011**). Crystal structure determination of the silver carboxylate dimer $[Ag(O_2C_{22}H_{43})]_2$, silver behenate, using powder X-ray diffraction methods," Powder Diff. **26**, 313–320.

Bruker AXS (**2005**). *TOPAS V3: General Profile and Structure Analysis Software for Powder Diffraction Data – Users Manual* (Bruker AXS Inc., Karlsruhe, Germany).

Chen, X. M., and Mak, T. C. W. (**1991**). "Metal-betaine interactions – VIII. Crystal structure of catena-(pyridine betaine)(nitrato)silver(I), $[Ag(C_5H_5NCH_2COO)(NO_3)]_n$," Polyhedron **10**, 1723–1726.

Clark, S. J., Segal, M. D., Pickard, C. J., Hasnip, P. J., Probert, M. J., Refson, K., and Payne, M. C. (**2005**). "First principles methods using CASTEP," Z. Krist. **220**, 567–570.

Coelho, A. (**2007**). *TOPAS-Academic V4* (Coelho Software, Brisbane, Australia). Available at http://www.topas-academic.net

Cowdery-Corvan, P. J. and Whitcomb, D. R. (**2002**). "Photothermographic and thermographic imaging materials," in *Handbook of Imaging Materials*, edited by A. Diamond (Marcel Dekker Inc., New York), 2nd ed., pp. 473–529.

David, W. I. F., Shankland, K., and Shankland, N. (**1998**). "Routine determination of molecular crystal structures from powder diffraction data," Chem. Commun. **8**, 931–932.

Jaber, F., Charbonnier, F., Petit-Ramel, M., and Faure, R. (**1996**). "A new silver(I) carboxylate chelate type: a six-membered ring in the N-oxide-picolinate," Eur. J. Solid State Inorg. Chem. **33**, 429–440.

Lee, S. J., Han, S. W., Choi, H. J., and Kim, K. (**2002**). "Structure and thermal behavior of a layered silver carboxylate," J. Phys. Chem. B **106**, 2892–2900.

Morgan, D. A. (**1991**). "Dry silver photographic materials," in *Handbook of Imaging Materials*, edited by A. Diamond (Marcel Dekker Inc., New York), pp. 43–60.

Olson, L. P., Whitcomb, D. R., Rajeswaran, M., and Stwertka, B. J. (**2006**). "The role of the Ag–Ag bond in the formation of silver nano-particles during the thermally induced reduction of silver carboxylates," Chem. Mater. **18**, 1667–1674.

Pagola, S., and Stephens, P. W. (**2010**). "*PSSP*, a computer program for the crystal structure solution of molecular materials from X-ray powder diffraction data," J. Appl. Cryst. **43**, 370–376.

Pawley, G. S. (**1991**). "Unit-cell refinement from powder diffraction scans," J. Appl. Cryst. **14**, 357–367.

Whitcomb, D. R. and Rajeswaran, M. (**2006**). "Designing silver carboxylate polymers: crystal structures of silver-acetyl-benzoate and silver-1,2-benzenedicarboxylate monomethyl ester," Polyhedron **25**, 1747–1752.

Wu, D. D. and Mak, T. C. W. (**1995**). "Building two-dimensional silver (I) co-ordination polymers with dicarboxylate-like ligands: Synthesis and crystal structures of polymeric complexes of silver nitrate and perchlorate with flexible double betaines," J. Chem. Soc. Dalton Trans. **16**, 2671–2678.